ELSEVIER

Physica A 293 (2001) 385–404

PHYSICA A

www.elsevier.com/locate/physa

Hydrodynamic modes of a three-dimensional sheared granular material

V. Kumaran*

Department of Chemical Engineering, Indian Institute of Science, Bangalore 560 012 India

Received 2 May 2000

Abstract

The hydrodynamic modes of a three-dimensional sheared granular flow are determined by solving the linearised Boltzmann equation. The steady state is determined using an expansion in the parameter $\varepsilon = (1 - e)^{1/2}$, and terms correct to $O(\varepsilon^4)$ are retained in the expansion. The distribution function is expressed as the product of a Gaussian distribution and an expansion in Hermite polynomials, and the coefficients in the expansion are determined by solving the Boltzmann equation for the steady flow. A basis set consisting of 14 functions, containing products of Hermite polynomials upto fourth order, were used for calculating the steady distribution function. In order to determine the decay rate of the hydrodynamic modes, small perturbations in the form of Fourier modes in the spatial directions and a Hermite polynomial expansion in the particle velocities, were placed on the base state, and the initial growth rates of these perturbations were determined. The number of solutions for the initial growth rates depend on the number of basis functions used for defining the perturbations. However, it was found that the initial growth rates of the hydrodynamic modes showed small variations when the number of basis functions was increased from 10 to 20. The initial growth rates for the hydrodynamic modes showed unusual behaviour in the flow and the vorticity directions. In the flow directions, the scaling laws previously obtained for a two-dimensional system were recovered in this case as well. In the vorticity direction, it was found that all five growth rates were real, and proportional to m in the limit $m \to 0$, where m is the wave number in the vorticity direction. In addition, two of the growth rates are positive, indicating that there are two unstable modes in this direction.

PACS: 05.20; 46.01+z; 62.90+k

Keywords: Granular materials; Shear flow; Hydrodynamic modes; Boltzmann equation

* Tel.: +91-80-309-2769; fax: +91-80-360-0683.
E-mail address: kumaran@chemeng.iisc.ernet.in (V. Kumaran).

0378-4371/01/$ - see front matter
PII: S0378-4371(00)00589-6

1. Introduction

The homogeneous shear flow of a granular material is a widely studied example of a driven dissipative system, where there is a balance between the source of energy due to the mean shear and the dissipation of energy due to inelastic collisions between particles. It is natural to draw an analogy between the motion of the particles in the shear flow, and that of molecules in a gas, and kinetic theory techniques [1–4] have been used to obtain macroscopic equations for the homogeneous sheared granular flow. The method used is similar to the derivation of the Navier–Stokes equation for a hard sphere gas from the Boltzmann equation using the Chapman–Enskog theory. The resultant equations are similar to that for a gas at equilibrium, with an additional energy dissipation term due to inelastic collisions. Kinetic theory techniques have also been used to determine the boundary conditions for the shear flow [5]. Approximate methods for determining the distribution function using the revised Enskog expansion have also been developed [6,7]. In recent years, another system that has received attention is the homogeneous cooling state of a granular gas. The homogeneous state of the system has been studied [8,9], and the hydrodynamic modes have also been determined [10].

There have been many studies on the stability of the homogeneous sheared state of the granular material. The earliest results were obtained by computer simulations [11], which indicated that the homogeneous sheared state of the material is unstable to density perturbations. The stability of a homogeneous sheared state to perturbations in the direction perpendicular to the mean velocity was first analysed by Mello et al. [12]. Subsequent studies by Savage [13] and Babic [14] considered perturbations in the flow as well as the gradient directions. Using a continuum description based on the mass, momentum and energy conservation equations, a linear stability analysis was used to determine the growth rate of perturbations. Both these studies indicated that the sheared state is unstable for a wide range of parameter values. Subsequent studies [15,16] used a more sophisticated stability analysis where the wave vector of the disturbances were considered to be a function of time, and the wave vector was considered to be turning with the flow. In these studies, the evolution of a suitably defined norm of the disturbance field was analysed to determine the stability of the system. These studies indicated that though the homogeneous sheared state is linearly unstable, the norm of the disturbance field could still bounded at long times after transients decay, and the homogeneous state could still be stable at long times. All of these studies used a continuum description of the granular flow.

In earlier studies by the author, the Boltzmann equation was used as the starting point for determining the steady distribution function and the growth rate of the hydrodynamic modes. The steady distribution for a homogeneous shear flow and a wall bounded shear flow were determined using a Hermite polynomial expansion starting from the Boltzmann equation [17]. The hydrodynamic modes of a two-dimensional sheared granular material for this steady distribution was studied [18] using the Boltzmann equation as the starting point. The base state was considered as the product of a Gaussian distribution and an expansion in a Hermite polynomial series, and

the coefficients of the terms in the series were determined using an expansion in the parameter $\varepsilon = (1-e)^{1/2}$. Terms correct to $O(\varepsilon^4)$ were retained in the expansion. The initial growth rates of the hydrodynamic modes were determined by placing small perturbations on the base flow in the form of Fourier modes in the spatial directions and a Hermite polynomial expansion in the particle velocities. The results indicated that the hydrodynamic modes show unusual behaviour for perturbations in the flow direction. In particular, there one mode, corresponding to the transverse momentum in an elastic system, which has a positive growth rate indicating that this mode is unstable in the long wavelength limit. The growth rate of this mode increases proportional to $|k|^{2/3}$ in the limit $k \to 0$, where k is the wave vector in the flow direction. The real and imaginary parts of the propagating modes also show the $|k|^{2/3}$ behaviour in the limit $k \to 0$, while the mode corresponding to energy fluctuations is damped.

Since unusual behaviour is exhibited by the hydrodynamic modes in a two-dimensional system, it is of interest to examine whether a three-dimensional sheared granular flow also exhibits similar behaviour. It is also of interest to examine the scaling of the modes in the vorticity direction, perpendicular to the plane of flow and velocity gradient, since this cannot be examined in a two-dimensional system. An analysis of the hydrodynamic modes for a three-dimensional sheared granular flow starting from the Boltzmann equation is carried out in the present paper.

2. Steady velocity distribution

The calculation of the steady velocity distribution is similar to that for a two-dimensional system, and so only a brief description is provided here. The system consists of rigid spherical particles undergoing a steady shear flow. The energy source is provided by the mean shear, and energy is dissipated due to inelastic collisions between the particles. The collisions are modeled with a constant coefficient of restitution e which is independent of the relative velocity of the particles. A Cartesian coordinate system is used, where the mean velocity and velocity gradient are in the x and y directions, respectively, and the vorticity vector is in the z direction. The non-dimensional velocity and length scales are defined as $\mathbf{u} = (\mathbf{U}/T^{1/2})$ and $\mathbf{x} = \mathbf{X}/(nd^2)^{-1}$, where $\mathbf{U}$ is the dimensional 'peculiar' velocity, which is the difference between the particle velocity and the mean velocity, and $\mathbf{X}$ is the dimensional position vector, and n and d are the number density and diameter of the particles. The dimensional mean velocity is defined as $\mathbf{U}_m = \Gamma Y \mathbf{e}_x$, where $\mathbf{e}_x$ is the unit vector in the x direction. The scaled strain rate, which is the rate of change of the mean velocity in the x velocity with the y coordinate, then becomes $\gamma = \Gamma/(nd^2T^{1/2})$, where Γ is the dimensional strain rate. The analysis proceeds with the definition of the velocity distribution function, $f(\mathbf{x},\mathbf{u},t)$, such that $f(\mathbf{x},\mathbf{u},t)\,\mathrm{d}\mathbf{x}\,\mathrm{d}\mathbf{u}$ is the number of particles in the differential volume $\mathrm{d}\mathbf{x}$ about $\mathbf{x}$ in real space and $\mathrm{d}\mathbf{u}$ about $\mathbf{u}$ in velocity space. For a steady homogeneous flow, $f(\mathbf{x},\mathbf{u},t) = F(\mathbf{u})$ is only a function of particle velocity. The Boltzmann equation for the distribution function at steady state in the absence of

spatial gradients is

$$-\gamma\frac{\partial u_y F(\mathbf{u})}{\partial u_x} = \frac{\partial_c F(\mathbf{u})}{\partial t}\,, \tag{1}$$

where the collision integral is

$$\frac{\partial_c F(\mathbf{u})}{\partial t} = \int_{\mathbf{u}^*}\int_{\mathbf{a}} (e^{-2}F(\mathbf{u}_b)F(\mathbf{u}_b^*) - F(\mathbf{u})F(\mathbf{u}^*))\mathbf{w}.\mathbf{a}\,, \tag{2}$$

where $\int_{\mathbf{u}^*} \equiv \int \mathrm{d}\mathbf{u}^*$ and $\int_{\mathbf{a}} \equiv \int \mathrm{d}\mathbf{a}$. In the equation 1, the velocity u_i is the velocity *relative* to the mean flow velocity. In Eq. (2), $\mathbf{u}_b$ and $\mathbf{u}_b^*$ are the velocities of a pair of particles before collision so that the post collisional velocities are $\mathbf{u}$ and $\mathbf{u}^*$, $\mathbf{a}$ is the unit vector in the direction of the line joining the centers of particles at collision, $\mathbf{w} = \mathbf{u} - \mathbf{u}^*$ is the velocity difference between the particles, and the above integral is carried out for $\mathbf{w}.\mathbf{a} \geqslant 0$ so that the particles approach each other prior to collisions. The factor e^{-2} in the first term of the above equation accounts for the contraction of phase space in a collision due to the inelastic nature of the collision between particles.

An expansion of the form

$$F(\mathbf{u}) = F_0(\mathbf{u})\left[1 + \sum_{n=1}^{I} A_i\phi_i(\mathbf{u})\right]\,, \tag{3}$$

where $F_0(\mathbf{u})$ is the Maxwell–Boltzmann distribution

$$F_0(\mathbf{u}) = \left(\frac{1}{2\pi}\right)^{3/2}\exp\left(-\frac{u^2}{2}\right) \tag{4}$$

is used for calculating the distribution function, where the basis functions ϕ_i are chosen as follows. If an index N is chosen such that polynomials of order $u_x^n u_y^{p-n} u_z^{N-p}$ (for $n \leqslant p$ and $p \leqslant N$) and of lower order are retained in the expansion, the total number of terms in the expansion is I. Only even values of p and $(N-p)$ are used in the expansion for the base state, because the distribution function has to satisfy the symmetries $f(-u_x,-u_y,u_z) = f(u_x,u_y,u_z)$ and $f(u_x,u_y,-u_z) = f(u_x,u_y,u_z)$. Of these, it is necessary to consider the eigenfunctions for the mass and energy separately

$$\phi_{I-1} = (u_x^2 + u_y^2 + u_z^2 - 3)/\sqrt{6}\,,$$

$$\phi_I = 1 \tag{5}$$

since these are collisional invariants. The other basis functions, ϕ_1 to ϕ_{I-2}, are defined as

$$\phi_i(u_x,u_y,u_z) = He_n(u_x)He_{p-n}(u_y)He_{q-p}(u_z)/|He_n(u_x)He_{p-n}(u_y)He_{q-p}(u_z)| \tag{6}$$

for $p = 2,4,6,\ldots,l$ and $q = 0,2,\ldots,N$, and the norm $|\ldots|$ is defined as

$$|He_n(u_x)He_{p-n}(u_y)He_{q-p}(u_z)| = \int_{-\infty}^{\infty}\mathrm{d}u_x\int_{-\infty}^{\infty}\mathrm{d}u_y\int_{-\infty}^{\infty}\mathrm{d}u_z\left(\frac{1}{2\pi}\right)^{3/2}$$
$$\times\exp\left(-\frac{u_x^2+u_y^2+u_z^2}{2}\right)He_n(u_x)He_{p-n}(u_y)He_{q-p}(u_z)\,. \tag{7}$$

The above norm ensures that the functions ϕ_i have the following property:

$$|\phi_i\phi_j| = 1 \quad \text{for } i = j\,, \tag{8}$$

$$= 0 \quad \text{for } i \neq j\,. \tag{9}$$

In expansion 3, the coefficients A_{I-1} and A_I can be set equal to zero without loss of generality, since the basis functions corresponding to these coefficients are the mass and energy. It is appropriate to use a Hermite polynomial expansion because they form a complete and orthogonal function space when the inner product is defined with a Gaussian distribution as the weighting function.

The expansion is inserted into the Boltzmann equation, multiplied by $F_0(\mathbf{u})\phi_j(\mathbf{u})$ and integrated over the velocity coordinates to obtain a non-linear vector equation of the form

$$-\gamma(H_i + G_{ij}A_j) = M_i + L_{ij}A_j + N_{ijk}A_jA_k \tag{10}$$

were summation is carried out over the repeated indices, the $I \times 1$ matrices H_i and M_i are

$$H_i = \int_{\mathbf{u}} \phi_i(\mathbf{u}) \frac{\partial(u_y F_0(\mathbf{u}))}{\partial u_x}\,, \tag{11}$$

$$M_i = \int_{\mathbf{u}} \int_{\mathbf{u}^*} \int_{\mathbf{a}} F_0(\mathbf{u})F_0(\mathbf{u}^*)(\phi_i(\mathbf{u}') - \phi_i(\mathbf{u}))\mathbf{w}.\mathbf{a} \tag{12}$$

the $I \times I$ matrices G_{ij} and L_{ij} are

$$G_{ij} = \int_{\mathbf{u}} \phi_i(\mathbf{u}) \frac{\partial(F_0(\mathbf{u})u_y\phi_j(\mathbf{u}))}{\partial u_x}\,, \tag{13}$$

$$L_{ij} = \int_{\mathbf{u}} \int_{\mathbf{u}^*} \int_{\mathbf{a}} F_0(\mathbf{u})F_0(\mathbf{u}^*)(\phi_j(\mathbf{u}) + \phi_j(\mathbf{u}^*))(\phi_i(\mathbf{u}') - \phi_i(\mathbf{u}))\mathbf{w}.\mathbf{a} \tag{14}$$

$$\tag{15}$$

and the third order tensor N_{ijk} is

$$N_{ijk} = \int_{\mathbf{u}} \int_{\mathbf{u}^*} \int_{\mathbf{a}} F_0(\mathbf{u})F_0(\mathbf{u}^*)\phi_j(\mathbf{u})\phi_k(\mathbf{u}^*)(\phi_i(\mathbf{u}') - \phi_i(\mathbf{u}))\mathbf{w}.\mathbf{a}\,, \tag{16}$$

where $\mathbf{u}'$ is the velocity after an inelastic collision of a particle which has a precollisional velocity $\mathbf{u}$ and collides with a particle with velocity $\mathbf{u}^*$ with the unit vector along the line of centers given by $\mathbf{a}$.

The coefficients A_i and the shear rate γ are obtained using an asymptotic expansion in the parameter $\varepsilon = (1-e)^{1/2}$ in the limit $(1-e) \ll 1$, and terms upto $O(\varepsilon^4)$ are retained in the expansion. The scaled shear rate is expanded as

$$\gamma = \varepsilon\gamma^{(1)} + \varepsilon^2\gamma^{(2)} + \varepsilon^3\gamma^{(3)} + \varepsilon^4\gamma^{(4)} \tag{17}$$

while the coefficients A_i are expressed as

$$A_i = \varepsilon A_i^{(1)} + \varepsilon^2 A_i^{(2)} + \varepsilon^3 A_i^{(3)} + \varepsilon^4 A_i^{(4)} \tag{18}$$

Table 1

	$K=5$	$K=14$
γ	$6.34133\varepsilon - 0.72392\varepsilon^3$	$6.29475\varepsilon + 2.46542\varepsilon^3$
$\langle u_x u_y \rangle$	$-1.11803\varepsilon + 0.36151\varepsilon^3$	$-1.12631\varepsilon + 0.85694\varepsilon^3$
$\langle u_x^2 - u_y^2 \rangle$	$1.25\varepsilon^2 - 2.1546\varepsilon^4$	$2.5727\varepsilon^2 - 2.0174\varepsilon^4$
$\langle u_y^2 - u_z^2 \rangle$	$-0.0446\varepsilon^2 - 0.0125\varepsilon^4$	$-0.2090\varepsilon^2 + 0.1064\varepsilon^4$

Similarly, the matrices M_i, L_{ij} and N_{ijk} are also expanded in a series in the parameter ε

$$M_i = M_i^{(0)} + \varepsilon^2 M_i^{(2)} + \varepsilon^4 M_i^{(4)} + \cdots$$

$$L_{ij} = L_{ij}^{(0)} + \varepsilon^2 L_{ij}^{(2)} + \varepsilon^4 L_{ij}^{(4)} + \cdots$$

$$N_{ijk} = N_{ijk}^{(0)} + \varepsilon^2 N_{ijk}^{(2)} + \varepsilon^4 N_{ijk}^{(4)} + \cdots \tag{19}$$

In these series, only the terms corresponding to even powers of ε are non-zero because only powers of $(1-e)$ appear in these integrals. These series are inserted into Eq. (10) to obtain solutions for the shear rate and the coefficients $A_i^{(p)}$. The leading order equation is identically satisfied, since the Maxwell–Boltzmann distribution is a solution of the elastic collision operator. The $O(\varepsilon)$ equation is

$$-\gamma^{(1)} H_i = L_{ij}^{(0)} A_j^{(1)} . \tag{20}$$

This provides the coefficients $A_i^{(1)}$ in terms of the leading order strain rate $\gamma^{(1)}$ for $i=(1,I-2)$. Equations for $i=(I-1,I)$ are identically satisfied at this order. Note that the strain rate $\gamma^{(1)}$ is as yet unspecified. This is provided by the $O(\varepsilon^2)$ correction to the energy equation (for $i=I-1$). It can easily be verified that $H_{I-1}=0$, and $N_{(I-1)jl}^{(0)} = L_{(I-1)j}^{(0)} = 0$ for all j,l. Consequently, the leading order energy equation simplifies to

$$\gamma_1 G_{(I-1)j} A_j^{(1)} + M_{I-1}^{(2)} = 0 . \tag{21}$$

A similar procedure is used for determining the higher corrections to the distribution function.

The corrections to the distribution function have been obtained correct to $O(\varepsilon^4)$ or $(1-e)^2$ in the asymptotic expansion. Two sets of basis functions, one for $I=5$ corresponding to all moments upto second order (of the form $u_x^n u_y^{m-n} u_z^{2-m}$ for $0 \leqslant n \leqslant m \leqslant 2$) and one for $I=14$ corresponding to all moments upto fourth order (of the form $u_x^n u_y^{m-n} u_z^{4-m}$ for $0 \leqslant n \leqslant m \leqslant 4$) have been used. The results of the calculation are shown in Table 1. It is seen that the results for the shear rate and the moments of the velocity are in good agreement upto for $I=5$ and $I=14$ upto $O(\varepsilon^2)$, though there is some variation for the $O(\varepsilon^3)$ contributions. This indicates that truncation at second moments is not sufficient to capture the $O(\varepsilon^3)$ contribution to the distribution function, and a larger set of moments may be necessary. The results for $I=14$ are for calculating the decay rate of perturbations in the next section.

3. Dispersion relations

To calculate the dispersion relations, perturbations are imposed on the distribution function of the form

$$f(\mathbf{x},\mathbf{u},t) = F(\mathbf{u}) + f'(\mathbf{x},\mathbf{u},t)\,, \tag{22}$$

where the perturbation $f'(\mathbf{x},\mathbf{u},t)$ has the form

$$f'(\mathbf{x},\mathbf{u},t) = f^{\dagger}(t,\mathbf{u})\exp(\imath kx + \imath l y + \imath mz)\,, \tag{23}$$

where k, l and m are the wave numbers in the x (flow), y (gradient) and z (vorticity) directions, respectively. The linear variation of the mean velocity with the y coordinate results in a convective term in the Boltzmann equation which is a linear function of this coordinate, and so it is not possible to obtain an eigenvalue problem for the growth rate. This complication is resolved by a transformation where the wave vector rotates with the mean flow. In this case, the components of the wave vector are written as $k(t) = k(0)$, $l(t) = l(0) - \gamma k(0)$ and $m(t) = m(0)$. After this transformation is effected, the growth rate at the initial time ($t = 0$) is determined using the transformation

$$f^{\dagger}(t,\mathbf{u}) = \tilde{f}(\mathbf{u})\exp(st)\,, \tag{24}$$

where s is the initial growth rate. The above form of the distribution function is inserted into the Boltzmann equation, and linearised about the base state to obtain an equation for the form

$$(s + \imath k u_x + \imath l u_y + \imath m u_z)\tilde{f} - \gamma\frac{\partial u_y \tilde{f}}{\partial u_x} = \frac{\partial_{cl}\tilde{f}}{\partial t}\,, \tag{25}$$

where the linearised collision integral is given by

$$\frac{\partial_{cl}\tilde{f}}{\partial t} = \int_{\mathbf{u}^*}\int_{\mathbf{a}}\left(\frac{1}{e^2}(F(\mathbf{u}_b)\tilde{f}(\mathbf{u}_b^*) + F(\mathbf{u}_b^*)\tilde{f}(\mathbf{u}_b)) - F(\mathbf{u})\tilde{f}(\mathbf{u}^*) - F(\mathbf{u}^*)\tilde{f}(\mathbf{u})\right)\mathbf{w}.\mathbf{a}\,. \tag{26}$$

A series of the following form is assumed for the perturbation to the distribution function $\tilde{f}$:

$$\tilde{f}(\mathbf{u}) = F_0(\mathbf{u})\sum_{i=1}^{J}\tilde{A}_i\phi_i\,, \tag{27}$$

where the basis functions ϕ_i were defined in Eqs. (5) and (6). This series is inserted into Eq. (25), multiplied by the basis function $\phi_i(\mathbf{u})$ and integrated over the particle velocities to get the following matrix equation:

$$(sI_{ij} + \imath kX_{ij} + \imath lY_{ij} + \imath mZ_{ij} - \gamma G_{ij} - C_{ij})\tilde{A}_j = M_{ij}\tilde{A}_j = 0\,, \tag{28}$$

where I_{ij} is the identity matrix, and the other matrices are defined as

$$X_{ij} = \int_{\mathbf{u}} F_0(\mathbf{u})u_x\phi_i(\mathbf{u})\phi_j(\mathbf{u})\,, \tag{29}$$

$$Y_{ij} = \int_{\mathbf{u}} F_0(\mathbf{u}) u_y \phi_i(\mathbf{u}) \phi_j(\mathbf{u}) \,, \tag{30}$$

$$Z_{ij} = \int_{\mathbf{u}} F_0(\mathbf{u}) u_z \phi_i(\mathbf{u}) \phi_j(\mathbf{u}) \,, \tag{31}$$

$$G_{ij} = \int_{\mathbf{u}} F_0(\mathbf{u}) \phi_i(\mathbf{u}) \left(\frac{\partial u_y \phi_j(\mathbf{u})}{\partial u_x} - u_y u_x \phi_j \right) \,, \tag{32}$$

$$C_{ij} = \sum_{k=1}^{K} A_k \int_{\mathbf{u}} \int_{\mathbf{u}^*} \int_{\mathbf{a}} F_0(\mathbf{u}) F_0(\mathbf{u}^*) (\phi_k(\mathbf{u}) \phi_j(\mathbf{u}^*) + \phi_k(\mathbf{u}^*) \phi_j(\mathbf{u})) (\phi_i(\mathbf{u}') - \phi_i(\mathbf{u})) (\mathbf{w}.\mathbf{a}) \,. \tag{33}$$

The dispersion relation is obtained by setting the determinant of the matrix M_{ij} equal to zero, so that there are non-trivial solutions for the amplitudes $\tilde{A}_j$.

The values of J in 27, the total number of basis functions used, were $J = 10$ (corresponding to all moments of the type $u_x^i u_y^{j-i} u_z^{2-j}$ for $i \leqslant j \leqslant 2$) and $J = 20$ (corresponding to all moments of the type $u_x^i u_y^{j-i} u_z^{3-j}$ for $i \leqslant j \leqslant 3$). It was found that though the set of eigenvalues for the dispersion matrix depended on the number of basis functions used, the eigenvalues for the hydrodynamic modes (which have zero decay rates in a homogeneous elastic system) was relatively insensitive to the number of basis functions used. The results for a basis set consisting of 20 basis functions are presented in the next section. A comparison for the results obtained using 10 basis functions and 20 basis functions for $e = 0.7$ (the lowest value of elasticity used) is also provided, in order to show that the variation is small when the number of basis functions is increased from 10 to 20. For an elastic system, a set of 10 basis functions does not provide the correct expression for the energy decay rate, because third moments (which are responsible for the convection of energy) are not included in the description. Surprisingly, they do provide an accurate description for inelastic systems, as shown in the next section, because the energy mode is damped. The basis set consisting of 20 basis functions provides an accurate result for the decay rate of the energy mode.

4. Results

The results are first validated with those for an elastic system of particles where mass, momentum and energy are conserved variables. For a basis set consisting of I functions, there are I solutions for the growth rate. For a system of elastic particles [19], five of these correspond to the conserved mass, momenta and energy basis functions. In a homogeneous system ($k = 0$), the growth rate corresponding to these five basis functions is equal to zero, while all others are negative. For $k \neq 0$, the energy mode s_{d3} is diffusive, which implies that their growth rate is real, negative and proportional to k^2 in the limit $k \to 0$. The two transverse velocity modes s_{d1} and s_{d2} are also diffusive

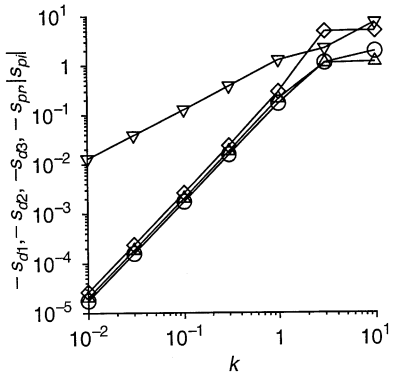

Fig. 1. Variation in the magnitudes of the growth rates of the hydrodynamic modes for a three dimensional gas of elastic particles: (○) $-s_{d1}, -s_{d2}$; (◇) $-s_{d3}$; (△) $-s_{pr}$; (▽) s_{pi}.

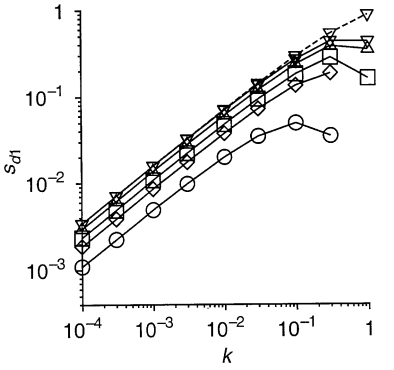

Fig. 2. Variation in s_{d1} as a function of k: (○) $e=0.99$; (◇) $e=0.95$; (□) $e=0.9$; (△) $e=0.8$; (▽) $e=0.7$. The broken line shows the result obtained using 10 basis functions for $e=0.7$.

and have equal damping rates. There are two modes corresponding to the propagation of sound which involve density and longitudinal momentum variations. The real part of the growth rates of these modes, s_{pr}, are negative and proportional to k^2, while the imaginary parts, s_{pi}, are equal in magnitude and opposite in sign and increase proportional to k in the limit $k \to 0$. The growth rates for the above hydrodynamic modes, obtained using a basis set consisting of 20 basis functions, are shown in Fig. 1. Note that the real parts of the growth rates for the hydrodynamic modes are negative, and their magnitudes are shown in Fig. 1.

The initial growth rates in the sheared state for inelastic particles depend on the wave vectors in the three directions, k, l and m. It is first useful to examine the dependence of the results when the number of basis functions is varied from 10 to 20. Figs. 2–6 show the variation in the initial growth rates of different modes for $e=0.7$ when the number of basis functions is changed from 10 to 20. It is observed that there is excellent agreement between the results even at the lowest value of the coefficient

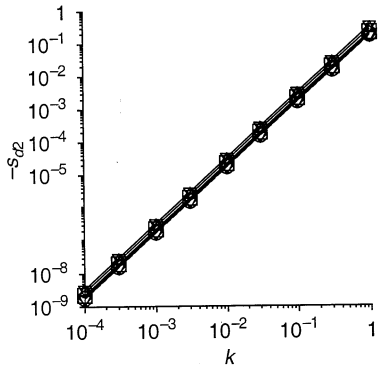

Fig. 3. Variation in $-s_{d2}$ as a function of k: (○) $e=0.99$; (◇) $e=0.95$; (□) $e=0.9$; (△) $e=0.8$; (▽) $e=0.7$. The broken line shows the result obtained using 10 basis functions for $e = 0.7$.

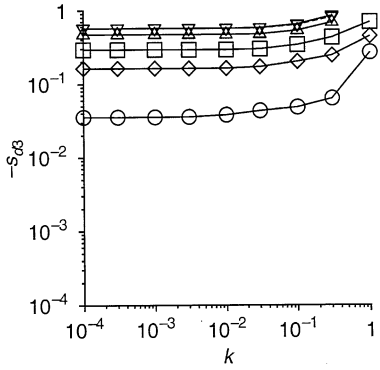

Fig. 4. Variation in $-s_{d3}$ as a function of k: (○) $e=0.99$; (◇) $e=0.95$; (□) $e=0.9$; (△) $e=0.8$; (▽) $e=0.7$. The broken line shows the result obtained using 10 basis functions for $e = 0.7$.

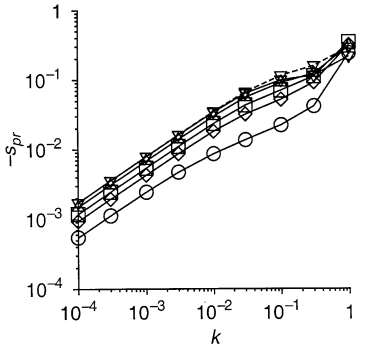

Fig. 5. Variation in $-s_{pr}$ as a function of k: (○) $e=0.99$; (◇) $e=0.95$; (□) $e=0.9$; (△) $e=0.8$; (▽) $e=0.7$. The broken line shows the result obtained using 10 basis functions for $e = 0.7$.

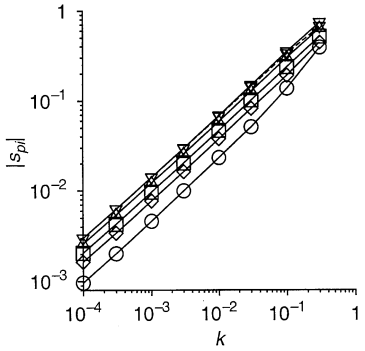

Fig. 6. Variation in $|s_{pi}|$ as a function of k: (○) $e=0.99$; (◇) $e=0.95$; (□)$e=0.9$; (△) $e=0.8$; (▽) $e=0.7$. The broken line shows the result obtained using 10 basis functions for $e=0.7$.

of restitution considered here. Consequently, the results reported below are obtained using a basis set consisting of 20 functions.

The growth rate for the perturbations in the flow directions as a function of wave number k for $l=0$ and $m=0$ have the following characteristics.

(1) As in the case of a two-dimensional sheared system, the growth rate for the least stable diffusive mode s_{d1} is real and *positive*. This confirms previous results that long wave length perturbations are *unstable* for modes with wave vector along the flow direction for three-dimensional sheared granular flows as well. The growth rate is plotted as a function of k in Fig. 2 for different values of the coefficient of restitution e. It can be seen that the scaling of the growth rate of the diffusive mode has the form

$$s_{d1} = s_{d1k}|k|^{2/3} \tag{34}$$

for $k \ll 1$, in contrast to the usual hydrodynamic scaling $s_{d1} \propto k^2$ for systems of elastic particles. The variation of the coefficient s_{d1k} with the coefficient of restitution is shown in Fig. 7. As in the two-dimensional case, the coefficient s_{d1k} scales as $(1-e)^{1/3}$ in the limit $(1-e) \ll 1$.

(2) The growth rate for second diffusive mode is negative, and scales as

$$s_{d2} = -s_{d2k}k^2 \tag{35}$$

as shown in Fig. 3. The coefficient s_{d2k} converges to the value expected for elastic systems in the limit $(1-e) \ll 1$, as shown in Fig. 7.

(3) The growth rate for the third diffusive mode, s_{d3}, is negative and converges to a finite value in the limit $k \to 0$, as shown in Fig. 4. This is because energy is no longer conserved in collisions. In the limit $(1-e) \ll 1$, the coefficient $s_{d3} \propto (1-e)$, as shown in Fig. 7.

(4) The real part of the growth rate for the propagating mode s_{pr} turns out to be negative, and $-s_{pr}$ is plotted as a function of k for different values of e in Fig. 5. It is observed here as well that the growth rate has the form

$$s_{pr} = -s_{prk}|k|^{2/3}\,, \tag{36}$$

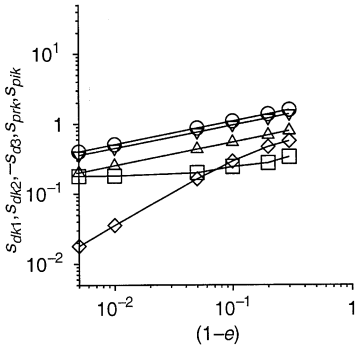

Fig. 7. The coefficients s_{d1k} (○), s_{d2k} (□), s_{prk} (△), s_{pik} (▽) and $-s_{d3}$ (◇) as a function of $(1-e)$ in the limit $k \to 0$.

where s_{prk}, which is a positive coefficient, is shown as a function of e in Fig. 7. This is in contrast to the k^2 scaling for elastic systems. Fig. 7 shows that s_{prk} increases with increase in $(1-e)$, and scales in a manner similar to s_{d1k}.

(5) The imaginary part of the growth rate for the propagating mode, s_{pi}, shown in Fig. 6, is also of the form

$$s_{pi} = \pm s_{pik}|k|^{2/3} \tag{37}$$

in contrast to the hydrodynamic scaling $s_{pi} \propto k$ in elastic systems. The coefficient s_{pik}, shown as a function of e in Fig. 7, also has a scaling similar to s_{d1k} and s_{prk}.

The behaviour of the growth rates as a function of l in the gradient direction at $k=0$ and $m=0$ are very similar to that for a two-dimensional system. Therefore, the results are just briefly mentioned here for completeness.

(1) The growth rates for two of the diffusive modes are negative and have the form

$$s_{d1} = -s_{d1l}l^2\,, \tag{38}$$

$$s_{d2} = -s_{d2l}l^2\,. \tag{39}$$

However, the coefficients s_{dl1} and s_{dl2} are different, unlike in the case of a homogeneous system where the growth rates of the two transverse velocity modes are identical. The variation of s_{d1l} and s_{d2l} with the parameter $(1-e)$ is shown in Fig. 8. It is observed that s_{d2l} converges to the value for an elastic system in the limit $(1-e) \ll 1$, but the coefficient s_{dl1} has a significantly different value even for $e=0.99$. This is in contrast to the two-dimensional case, where the coefficient of the least-stable diffusive mode decreased proportional to $(1-e)^2$ in the limit $(1-e) \ll 1$.

(2) The real and imaginary parts of the growth rate for the propagating modes, s_{pr} and s_{pi}, are of the form

$$s_{pr} = -s_{prl}l^2\,, \tag{40}$$

$$s_{pi} = \pm s_{pil}l\,. \tag{41}$$

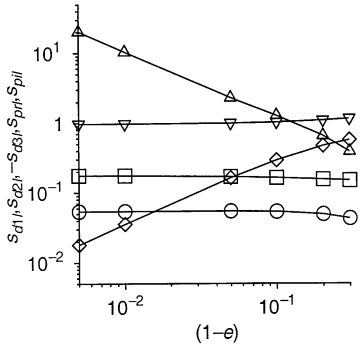

Fig. 8. The coefficients s_{d1l} (○), s_{d2l} (□), s_{prl} (△), s_{pil} (▽) and $-s_{d3}$ (◇) as a function of $(1-e)$ in the limit $k \to 0$.

Table 2

	$e=0.99,\ m=0.001$	$e=0.99,\ m=0.01$	$e=0.9,\ m=0.01$	$e=0.9,\ m=0.1$
s_1	1.217×10^{-3}	9.485×10^{-3}	1.166×10^{-2}	8.606×10^{-2}
s_2	3.045×10^{-5}	2.887×10^{-4}	8.707×10^{-4}	7.200×10^{-3}
s_3	-3.080×10^{5}	-2.255×10^{-2}	-9.041×10^{-4}	-0.1930
		$+9.309 \times 10^{-3}\imath$		$+0.1133\imath$
s_4	-1.309×10^{-3}	-2.255×10^{-2}	-1.274×10^{-2}	-0.1930
		$-9.309 \times 10^{-3}\imath$		$-0.1133\imath$
s_5	-3.546×10^{-2}	-3.401	-0.2925	-2.7564

A decrease in the coefficient of restitution increases the coefficient s_{prl}, thereby increasing the damping, and Fig. 8 indicates that s_{prl} increases proportional to $(1-e)^{-1}$ while s_{pil} tends to a constant value in the limit $(1-e) \ll 1$.

(3) The growth rate of the mode corresponding to total energy, s_{d3}, is damped because energy is not conserved in collisions. The variation of the growth rate in the limit $l \ll 1$, shown in Fig. 8, is similar to the variation of s_{d3} in the limit $k \ll 1$.

It should be noted that the scaling relations obtained from Figs. 7 and 8 are approximate, since it was not possible to extend the numerical results to $(1-e) < 0.01$ for reasons mentioned below.

The growth rate for perturbations in the vorticity direction as a function of wave number m at $k=0$ and $l=0$ have a more complicated behaviour. An example is shown in Table 2, where the growth rates for the hydrodynamic modes is shown as a function of m at different values of the coefficient of restitution. Two important inferences can be drawn

(1) There are *two unstable modes* which have growth rates with positive parts. This is in contrast to one unstable mode for variations in low direction $(l=0, m=0)$ and no unstable modes for variations gradient direction $(k=0, m=0)$. In addition, it can be seen two pairs of modes have growth rates of nearly equal magnitude positive signs.

(2) At a given coefficient of restitution, the growth rates of the hydrodynamic modes are all real for low values of m, indicating that there are no propagating modes in this

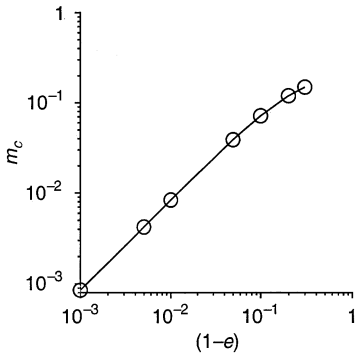

Fig. 9. Wave vector m_c for the cross over from five diffusive hydrodynamic modes of three diffusive and two propagating modes as a function of $(1-e)$.

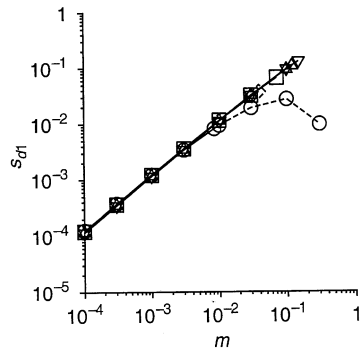

Fig. 10. Variation in s_{d1} as a function of m. The solid line shows the variation for $m < m_c$, and the broken line for $m > m_c$: (○) $e = 0.99$; (◇) $e = 0.95$; (□) $e = 0.9$; (△) $e = 0.8$; (▽) $e = 0.7$.

limit. As the wave number m is increased, is a cross over to the usual hydrodynamic behaviour where three growth rates are real (corresponding to the diffusive energy and transverse velocity modes), and the other two are complex and conjugate of each other (corresponding to the propagating sound modes). The value m_c for the cross over between these two types of behaviour shown as a function of $(1-e)$ in Fig. 9. It is seen that the value for the crossover decreases proportional to $(1-e)^{-1}$ in the limit $(1-e)\to 0$.

The behaviour of the hydrodynamic modes in the parameter regimes where there are five real growth rates are shown in Figs. 10–15.

(1) The two unstable modes have growth rates increasing proportional to m in the limit $m \ll 1$, as shown in Figs. 10 and 11.

$$s_{d1} = s_{d1m} m \,,$$

$$s_{d2} = s_{d2m} m \,. \tag{42}$$

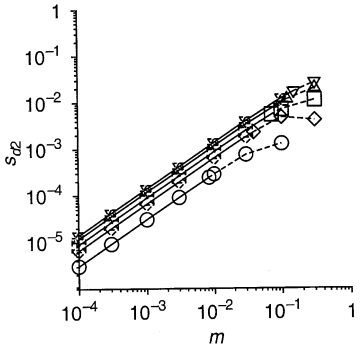

Fig. 11. Variation in s_{d2} as a function of m. The solid line shows the variation for $m < m_c$, and the broken line for $m > m_c$: (○) $e = 0.99$; (◇) $e = 0.95$; (□) $e = 0.9$; (△) $e = 0.8$; (▽) $e = 0.7$.

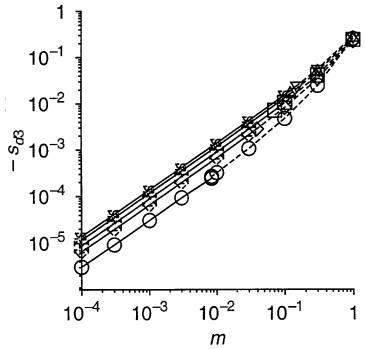

Fig. 12. Variation in $-s_{d3}$ as a function of m. The solid line shows the variation for $m < m_c$, and the broken line for $m > m_c$: (○) $e = 0.99$; (◇) $e = 0.95$; (□) $e = 0.9$; (△) $e = 0.8$; (▽) $e = 0.7$.

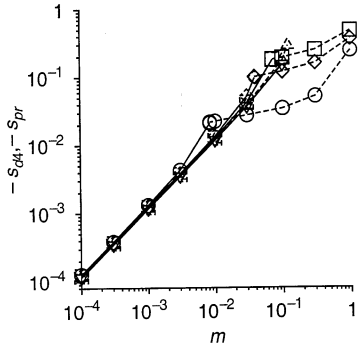

Fig. 13. Variation in $-s_{d4}$ (solid line) for $m < m_c$ and $-s_{pr}$ (broken line) for $m > m_c$ as a function of m: (○) $e = 0.99$; (◇) $e = 0.95$; (□) $e = 0.9$; (△) $e = 0.8$; (▽) $e = 0.7$.

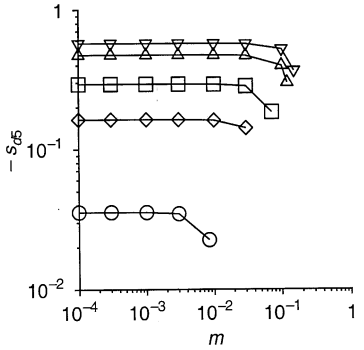

Fig. 14. Variation in $-s_{d5}$ as a function of m for $m < m_c$: (○) e=0.99; (◇) e=0.95; (□) e=0.9; (△) e=0.8; (▽) $e = 0.7$.

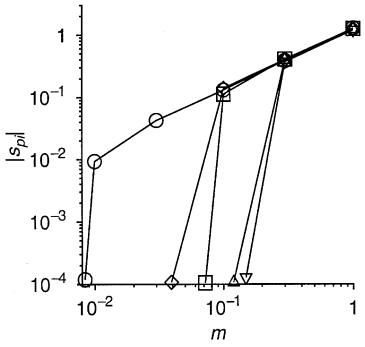

Fig. 15. Variation in $|s_{pi}|$ as a function of m for $m > m_c$: (○) e=0.99; (◇) e=0.95; (□) e=0.9; (△) e=0.8; (▽) $e = 0.7$.

The coefficients s_{d1m} and s_{d2m} are shown as a function of $(1 - e)$ in Fig. 16. It is observed that the coefficient s_{d1m} does not show much variation with $(1 - e)$, while the coefficient s_{d2m} decreases proportional to $(1 - e)^{1/2}$ in the limit $(1 - e) \to 0$.

(2) Two of the stable modes have growth rates which are negative, and which decrease proportional to m in the limit $m \ll 1$, as shown in Figs. 12 and 13.

$$s_{d3} = -s_{d3m}m\,,$$

$$s_{d4} = -s_{d4m}m\,. \tag{43}$$

It is observed from Fig. 16 that the scaling of s_{dm3} is the same as that of s_{dm2}, and the scaling of s_{dm4} is the same as that of s_{dm1}, though their numerical values are not exactly identical.

(3) The third stable mode s_{d5} has a finite negative value in the limit $m \to 0$, as shown in Fig. 14. Fig. 16 shows that this value decreases proportional to $(1 - e)$ in the limit $(1 - e) \ll 1$.

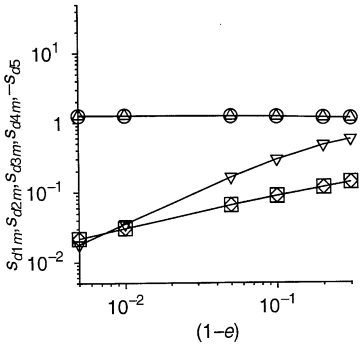

Fig. 16. The coefficients s_{d1m} (○), s_{d2m} (□), s_{d3m} (◇), s_{d4m} (△) and $-s_{d5}$ (▽) as a function of $(1-e)$ in the limit $k \to 0$.

It is also observed that the growth rates s_{d1}, s_{d2} and s_{d3} are continuous when there is a cross over at $m = m_c$ from five diffusive modes to three diffusive and two propagating modes. At $m = m_c$, s_{d4} and s_{d5} become equal, and two propagating modes appear for $m > m_c$. The real part of the growth rate of the propagating mode, shown in Fig. 13 for $m > m_c$, has a magnitude equal to s_{d4} and s_{d5} at $m = m_c$. The imaginary part, shown in Fig. 15, increases proportional to $(m - m_c)^{1/2}$ in the limit $(m - m_c) \ll m$.

As in the case of a two-dimensional system, the above results indicate that there is a qualitative change in the scaling of the hydrodynamic modes when the coefficient of restitution is changed from 1.0 to 0.99. It was shown [18] that the change in the scaling of the growth rates with the wave number k in the velocity direction is continuous, and there is no discontinuous change in the scaling behaviour. A similar feature is observed for the three-dimensional system as well.

5. Conclusions

The behaviour of the hydrodynamic modes of a three-dimensional sheared granular material have been examined as a function of the coefficient of restitution of the particles. In the steady state, there is a source of energy due to the mean shear flow, and energy dissipation due to inelastic collisions between the particles. The particle size is considered to be small compared to be the mean free path, so that the mean free path $1/(nd^2)$ is the only length scale in the problem, where n is the number density and d is the particle diameter. The only time scale is the strain rate Γ of the mean flow, and the mean square velocity of the particles is related to the strain rate from the energy conservation condition which requires that the source of energy due to the mean flow is equal to the dissipation due to inelastic collisions. The lengths are non-dimensionalised by the mean free path, and the velocity by the $T^{1/2}$, where T is the mean-square velocity of the particles, and the resulting dimensionless Boltzmann equation for the velocity distribution function depends only on the

coefficient of restitution e. The steady distribution function is expressed as the product of the Gaussian distribution and a series expansion in Hermite polynomials. This expansion is inserted into the Boltzmann equation, and solved to determine the coefficients in the expansion. An asymptotic analysis in the small parameter $\varepsilon = (1-e)^{1/2}$ is used, and terms correct to $O(\varepsilon^4)$ are retained in the expansion. For the present calculation, a basis set consisting of 14 basis functions was used to define the steady distribution.

The growth rate of the hydrodynamic modes were obtained using a linear stability analysis, where small perturbations were placed on the mean flow and the growth rates of these perturbations were determined. The number of solutions for the growth rates depend on the number of basis functions retained in the expansion, but it was found that the solution for the growth rates for the hydrodynamic modes showed small variations when the number of basis functions was varied from 10 to 20. For an elastic system, there are five modes, the mass, three components of the momenta and energy, which have zero growth rates in a homogeneous system, because mass, momentum and energy are conserved in collisions. All other modes have negative growth rates, indicating that transients composed of these modes decay over time scales comparable to the collision frequency. In the limit of small wave length, the energy and the two transverse components of the momentum have diffusive behaviour, and the decay rate of these modes decays proportional to k^2 in the limit $k \to 0$. The longitudinal momentum and density are propagating modes, and the decay rates of these have a real part proportional to k^2 and an imaginary part proportional to k.

The behaviour of the hydrodynamic modes in a sheared granular material are qualitatively different from that in an elastic gas. It was shown earlier [18] for a two-dimensional system that the growth rates of perturbations with variation in the flow direction show unusual scaling with the wave number. A similar behaviour is observed in the three dimensional system.

(1) One of the diffusive modes corresponding to the transverse momentum has a growth rate which is real and positive, indicating that perturbations are unstable in this direction, and the growth rate increases proportional to $|k|^{2/3}$ in the limit $k \to 0$. This is in contrast to the k^2 behaviour for an elastic system.

(2) The second diffusive mode corresponding to the transverse momentum is negative and real, and scales proportional to k^2 in the limit $k \to 0$.

(3) The energy mode has a growth rate which is negative and finite in the limit $k \to 0$, since energy is dissipated in collisions between particles.

(4) The real part of the propagating modes is negative, indicating that these modes are stable in the limit $k \to 0$. In addition, it is also observed that the real and imaginary parts of the propagating modes also increase proportional to $|k|^{2/3}$ in the limit $k \to 0$.

The $|k|^{2/3}$ behaviour is due to the advection of the wave vector with the mean flow, and it was shown [18] for a simple convection diffusion equation with a mean shear that the decay rate of the concentration fluctuations scales as $|k|^{2/3}$ in the long time limit. It has also been observed in thermostatted systems [20] where there is a drag force on the particles which is proportional to the particle velocity.

The present analysis indicates that the behaviour of the hydrodynamic modes in the vorticity direction, perpendicular to the plane of shear, also show unusual behaviour as a function of the wave vector m in this direction. Some of the unusual features in this direction are

(1) For a given coefficient of restitution, the hydrodynamic modes are all real when the wave vector m is less than a cross over value m_c, and this cross over value $m_c \propto (1-e)$ in the limit $(1-e) \ll 1$. Above the cross over value, there are three real solutions and two complex solutions for the growth rate, as observed in elastic systems.

(2) Two of the real solutions are positive, indicating that there are two unstable modes in the vorticity direction.

(3) For $m < m_c$, the growth rate of four of the five hydrodynamic modes increase proportional to m in the limit $m \to 0$. The fifth mode converges to a finite value because energy is dissipated in inelastic collisions.

The unusual behaviour of the hydrodynamic modes in the vorticity direction do not seem to have been observed before. This could be of significance in real granular systems, because the analysis indicates that clustering takes place in both the flow as well as the vorticity directions. The vorticity direction appears to be the most unstable direction for the sheared granular flow, and the instability in this direction is not recovered in previous two-dimensional studies.

References

[1] J.T. Jenkins, S.B. Savage, A theory for rapid flow of identical, smooth, nearly elastic, spherical particles, J. Fluid Mech. 130 (1983) 187.
[2] C.K.K. Lun, S.B. Savage, D.J. Jeffrey, N. Chepurniy, Kinetic theories of granular flow: inelastic particles in a Couette flow and slightly inelastic particles in a general flow field, J. Fluid Mech. 140 (1984) 223.
[3] J.T. Jenkins, M.W. Richman, Grad's 13 moment system for a dense gas of inelastic particles, Arch. Ration. Mech. Anal. 87 (1985) 355.
[4] N. Sela, I. Goldhirsch, S.H. Noskowicz, Kinetic theoretical study of a simply sheared two dimensional granular gas to Burnett order, Phys. Fluids 8 (1996) 2337.
[5] J.T. Jenkins, M.W. Richman, Boundary conditions for plane flows of smooth, nearly elastic, circular disks, J. Fluid Mech. 171 (1986) 53.
[6] J.J. Brey, J.W. Dufty, C.S. Kim, A. Santos, Hydrodynamics for granular flow at low density, Phys. Rev. E 58 (1998) 4638.
[7] J.M. Montanero, V. Garzo, A. Santos, J.J. Brey, Kinetic theory of simple granular shear flows of smooth hard spheres, J. Fluid Mech. 389 (1999) 391.
[8] T.P.C. van Noije, M.H. Ernst, R. Brito, Spatial correlations in compressible granular flows, Phys. Rev. E 57 (1998) 4891.
[9] T.P.C. van Noije, M.H. Ernst, Velocity distributions in homogeneously cooling and heated granular fluids, Granular Matter 1 (1998) 57.
[10] S. McNamara, Hydrodynamic modes of a uniform granular medium, Phys. Fluids A 5 (1993) 3056.
[11] M.A. Hopkins, M.Y. Louge, Inelastic microstructure in rapid granular flows of smooth disks, Phys. Fluids A 3 (1991) 47.
[12] T.M. Mello, P.H. Diamond, H. Levine, Hydrodynamic modes of a granular shear flow, Phys. Fluids A 3 (1991) 2067.
[13] S.B. Savage, Instability of unbounded uniform granular shear flow, J. Fluid Mech. 241 (1992) 109.
[14] M. Babic, On the stability of rapid granular flows, J. Fluid Mech. 254 (1993) 127.
[15] P.J. Schmid, H.K. Kytomaa, Transient and asymptotic stability of a granular shear flow, J. Fluid Mech. 264 (1994) 255.

[16] C.-H. Wang, R. Jackson, S. Sundaresan, Stability of bounded rapid shear flows of a granular material, J. Fluid Mech. 308 (1996) 31.
[17] V. Kumaran, Asymptotic solution of the Boltzmann equation for the shear flow of smooth inelastic disks, Physica A 274 (2000) 483–504.
[18] V. Kumaran, Anomalous behaviour of hydrodynamic modes in the two dimensional shear flow of a granular material, Physica A, accepted for publication.
[19] P. Resibois, M. de Leener, Classical Kinetic Theory of Fluids, Wiley, New York, 1977.
[20] M. Lee, J.W. Dufty, Transport far from equilibrium: uniform shear flow, Phys. Rev. E 56 (1997) 1733–1745.